ELM Suppression and Pedestal Structure in I-Mode Plasmas

by

John Reel Walk, Jr.

Submitted to the Department of Nuclear Science and Engineering
in partial fulfillment of the requirements for the degree of
Doctor of Philosophy in Applied Plasma Physics

Author .....
Department of Nuclear Science and Engineering
July 12, 2014

Certified by .....
Jerry W. Hughes
Research Scientist, Plasma Science and Fusion Center
Thesis Supervisor

EXECUTIVE SUMMARY

The development of magnetic-confinement fusion into an economical form of power generation is characterized by two overarching and seemingly-contradictory requirements: first, a high level of energy confinement is necessary to reach the desired level of self-heating of the plasma by fusion products, and second, a low level of particle confinement to avoid the deleterious effects of accumulated impurities (both the helium "fusion ash" and eroded plasma-facing wall materials). The latter is particularly important for the high-Z impurities expected from the metal wall materials necessary for reactor-scale devices. A number of operating regimes, collectively termed *H-modes*, have been developed satisfying these requirements in varying degrees. These regimes are characterized by the formation of a *pedestal*, a region of steep gradient in density, temperature, and pressure at the plasma edge that acts as a transport barrier in the plasma. The structure introduces an additional constraint, however – the steep gradients act as a source of free energy for explosive Edge-Localized Modes (ELMs), which on reactor-scale devices drive transient heat loading and erosion damage in excess of material tolerances for plasma-facing surfaces.

As the width and height of the pedestal set a strong constraint on both global performance and stability against ELMs, a firm understanding of the physics governing the pedestal structure is essential for the extrapolation of high-performance regimes to ITER- and reactor-scale operation. This thesis contributes to the understanding of pedestal physics and high-performance operation in two key areas:

not sure how specific to be with cites

move these into sections, bullet results for each chapter?

PREDICTIVE ELMY H-MODE PHYSICS

ELMy H-mode is commonly accessible on major tokamak experiments, and is considered the baseline for operation on ITER [1]. However, as large, uncontrolled ELMs are incompatible with ITER or reactor operation, an understanding of the stability space for ELM suppression, mitigation, or avoidance is necessary. This thesis details the testing of the predictive EPED model to operation on Alcator C-Mod. These experiments significantly expanded the parameter range on which EPED has been tested, particularly across a broad range in magnetic fields on C-Mod, and at the highest thermal pressures of any existing tokamak, within a factor of ~ 2 of the target pedestal pressure for ITER. The methods developed in this analysis are subsequently applied to the examination of I-mode pedestals.

I-MODE PEDESTAL STRUCTURE, PERFORMANCE, & STABILITY

I-mode [2] is a novel high-performance regime pioneered on Alcator C-Mod, unique in that it develops an H-mode-like temperature pedestal and good energy confinement, without the accompanying density pedestal or suppression of particle transport. I-mode exhibits three highly attractive properties for a reactor regime:

1. the lack of a particle transport barrier maintains the desired level of impurity flushing from the plasma, naturally allowing stationary operation with low radiative losses
2. Energy confinement in I-mode degrades significantly more weakly with increased heating power compared to H-mode, a highly desirable result for fusion self-heated plasmas
3. I-mode appears to be inherently stable against large, deleterious ELMs, avoiding the need for externally-applied mitigation/suppression techniques

This thesis first details an empirical study of the pedestal structure in I-mode, particularly its response to fueling and heating power, and its impact on global confinement and performance. It then details a computational study of the I-mode pedestal with regards to ELM stability, using the physics techniques developed for ELMy H-modes.

The results in this thesis have been published in a number of peer-reviewed papers, both for the ELMy H-mode results [3] (also featuring in a multi-machine Joint Research Target [4]) and for I-mode [5].

ELMY H-MODES

The pedestal in ELMy H-mode is thought to be limited by two constraints: the onset of edge peeling-ballooning MHD instabilities, and

transport driven by kinetic-ballooning mode (KBM) turbulence [6]. Experimental observations on C-Mod are consistent with these constraints, particularly when the pedestal data is masked to time frames immediately preceding the ELM crashes – a practice that, despite diagnostic difficulties on C-Mod, produces data most closely corresponding to the pedestal structure at the point of ELM instability.

The pedestal width is well-described by the prediction based on KBM physics, which predicts for the width Δ_ψ (here defined as the average of the density and temperature pedestal widths in normalized poloidal flux space) the relation $\Delta_\psi = G(\nu^*, \varepsilon, ...)\beta_{p,ped}^{1/2}$, where $G(\nu^*, \varepsilon, ...)$ is a weakly-varying function of plasma shape, aspect ratio, collisionality, and other dimensionless parameters (fig. 1). This scale function is fitted to a value of $\langle G \rangle \approx 0.085$, consistent with observations on other devices. Over the range in width and $\beta_{p,ped}$ seen on C-Mod, the secondary dependences of the width (encoded in G) are negligible – the width is well-described by the simple $\Delta_\psi \sim \beta_{p,ped}^{1/2}$ scaling. Moreover, the width is not well-described by the predictions from neutral-penetration models (consistent with the highly opaque SOL on C-Mod) or models based on ion-orbit loss, predicting $\Delta \sim \rho_{i,pol}$, indicating that the KBM limit most accurately describes the pedestal width.

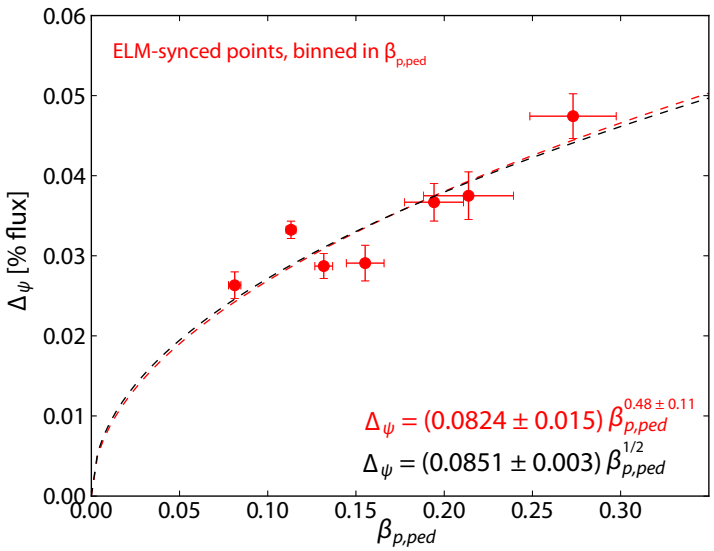

Figure 1: ELM-synchronized pedestals, with data binned by $\beta_{p,ped}$ for clarity. The data are fitted by $\Delta_\psi = (0.0851 \pm 0.003)\beta_{p,ped}^{1/2}$ (black) or by $\Delta_\psi = (0.0824 \pm 0.015)\beta_{p,ped}^{0.49 \pm 0.11}$ (red) using a more general power law.

The pressure profile is also consistent with the expected limit from peeling-ballooning MHD, particularly the $\nabla p \sim I_p^2$ expected from ideal ballooning modes. Taking the pressure pedestal height to scale as $p_{ped} \sim \nabla p \times \Delta_p$, the measured height trends as $I_p^2\sqrt{\beta_{p,ped}} \sim I_p\sqrt{n_{e,ped}T_{e,ped}}$ (fig. 2). With the fairly restricted range in both width and $\beta_{p,ped}$ typically seen on C-Mod due to the restricted, weak shaping needed for ELMy H-mode access, this reduces in the lowest order to a robust pedestal width with $p_{ped} \sim \nabla p \sim I_p^2$.

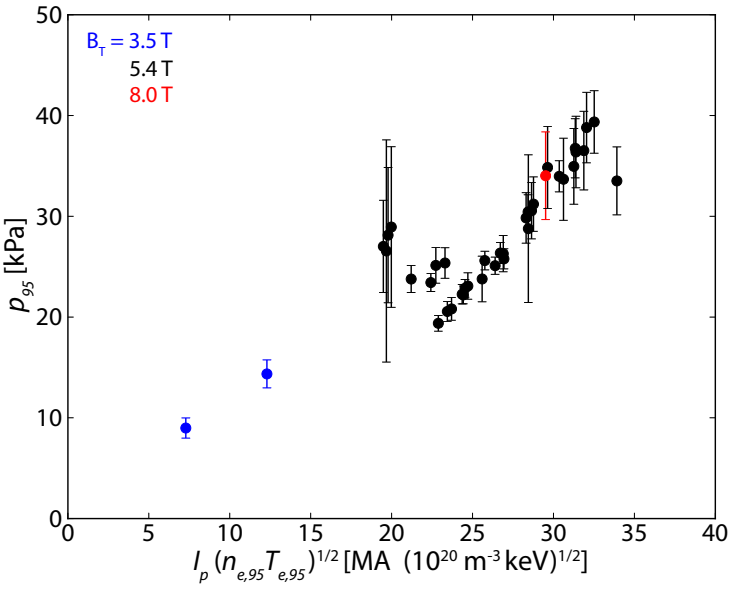

Figure 2: Pedestal pressure versus $I_p \sqrt{n_{e,95} T_{e,95}}$ – effectively, the $p_{ped} \sim I_p^2 \sqrt{\beta_{p,ped}}$ scaling predicted for a KBM-limited pedestal.

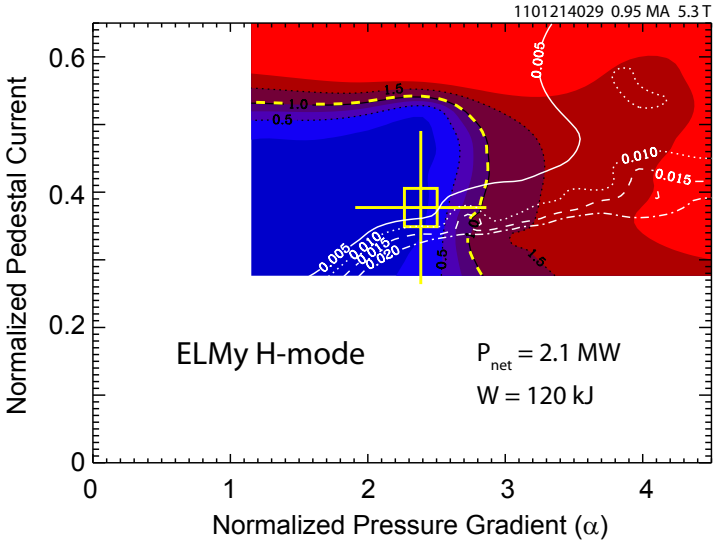

Figure 3: Calculation of the peeling-ballooning MHD stability contour from ELITE for an ELMy H-mode pedestal on C-Mod. The red-blue contours show the peeling-ballooning growth rate with diamagnetic stabilization, $\gamma/(\omega_{*eff}/2)$, while white contours show the width in flux space that is unstable to the KBM. To within error bars, the pedestal lies on the peeling-ballooning boundary. The comparatively higher collisionality typical of C-Mod H-mode pedestals pushes the MHD behavior of the pedestal towards higher-n, pure-ballooning modes, although moderate-n coupled modes in the "nose" of the stability contour are also common.

The peeling-ballooning MHD and KBM limits are examined in more detail using the ELITE and BALOO numerical codes (with the latter calculating the KBM threshold via an infinite-n ideal MHD surrogate), with results shown in fig. 3. These calculations are combined in the EPED model, particularly the most recent iteration, EPED1.63 (a minor modification to EPED1.6 to account for the strong diamagnetic stabilization effects expected for the pedestal on C-Mod). The EPED predictions for the pedestal height match well to observed pressure pedestals (to within the systematic ±20% error in EPED predictions), particularly when compared to measured pedestals masked to the ELM cycle as described above (see fig. 4), with an average ratio of measured to predicted pedestal pressure of 0.94 ± 0.066. While systematic tests of the predicted pedestal width against EPED pre-

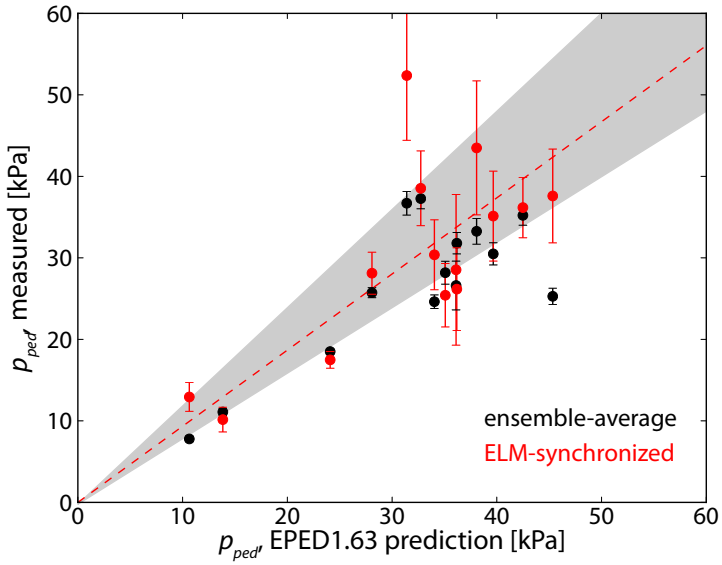

Figure 4: Pressure pedestal height predicted by EPED1.63 versus measured, ELM-synchronized pedestal height (with corresponding ensemble-averaged data shown in black). The grey band indicates agreement within the ±20% typical prediction accuracy for EPED. ELM synchronization brings the measured pedestal height into better agreement with EPED predictions, with a correspondence of 0.94 ± 0.066 (indicated by the red dash)

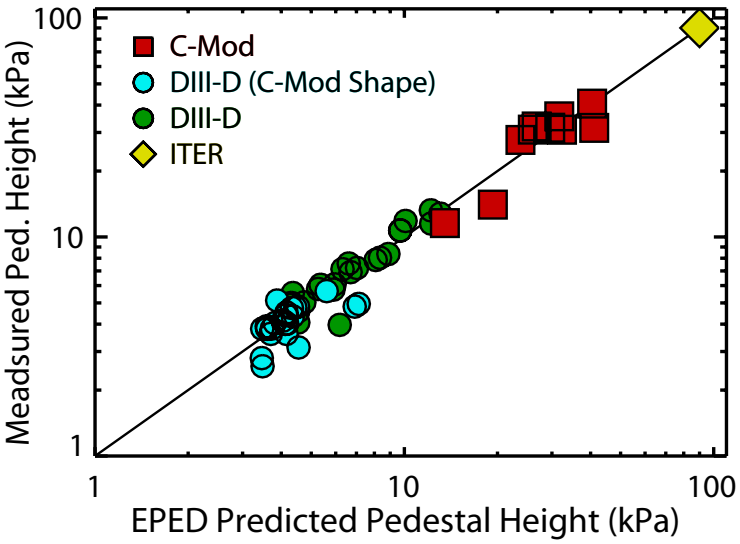

Figure 5: EPED predictions versus measured pressure pedestal heights from DIII-D and C-Mod, spanning a significant range of pedestal pressures. Notably, C-Mod pressure pedestals reach within a factor of ~ 2 of the predicted ITER pedestal height. Reproduced from [7]

dictions are difficult due to the narrow range over which the experimental Δ_ψ varies, EPED does reproduce the pedestal width to within ±20% while capturing the robustness of the pedestal width.

The experiments presented in this thesis greatly expanded the parameter range over which EPED has been tested, with magnetic field ranging over $3.5 - 8\,\mathrm{T}$ (reaching the highest field of any tokamak experiment), as well as reaching to within a factor of ~ 2 of the target pedestal thermal pressure for ITER (fig. 5). The ELMy H-mode is assumed to be the baseline high-performance scenario for ITER; moreover, the stability boundaries associated with the ELM trigger set upper bounds on the pedestal structure in other H-mode regimes. As such, a first-principles physics understanding of the ELM limit, as provided by EPED and thoroughly tested experimentally (including the work in this thesis), is essential for extrapolation of high-

confinement regimes to ITER. The analyses developed here for ELMy H-mode are subsequently applied to the understanding of I-mode pedestals.

I-mode pedestals & performance

Empirical observations of the I-mode pedestal structure are illuminating in terms of the observed global behavior in I-mode. The formation of a hot, H-mode-like temperature pedestal provides good energy confinement while naturally operating at ITER-relevant collisionality, while the absence of a density pedestal prevents the accumulation of impurities – particularly important for machines operating with high heat fluxes onto high-Z metal plasma-facing components, as is the case for C-Mod, and as expected for ITER.

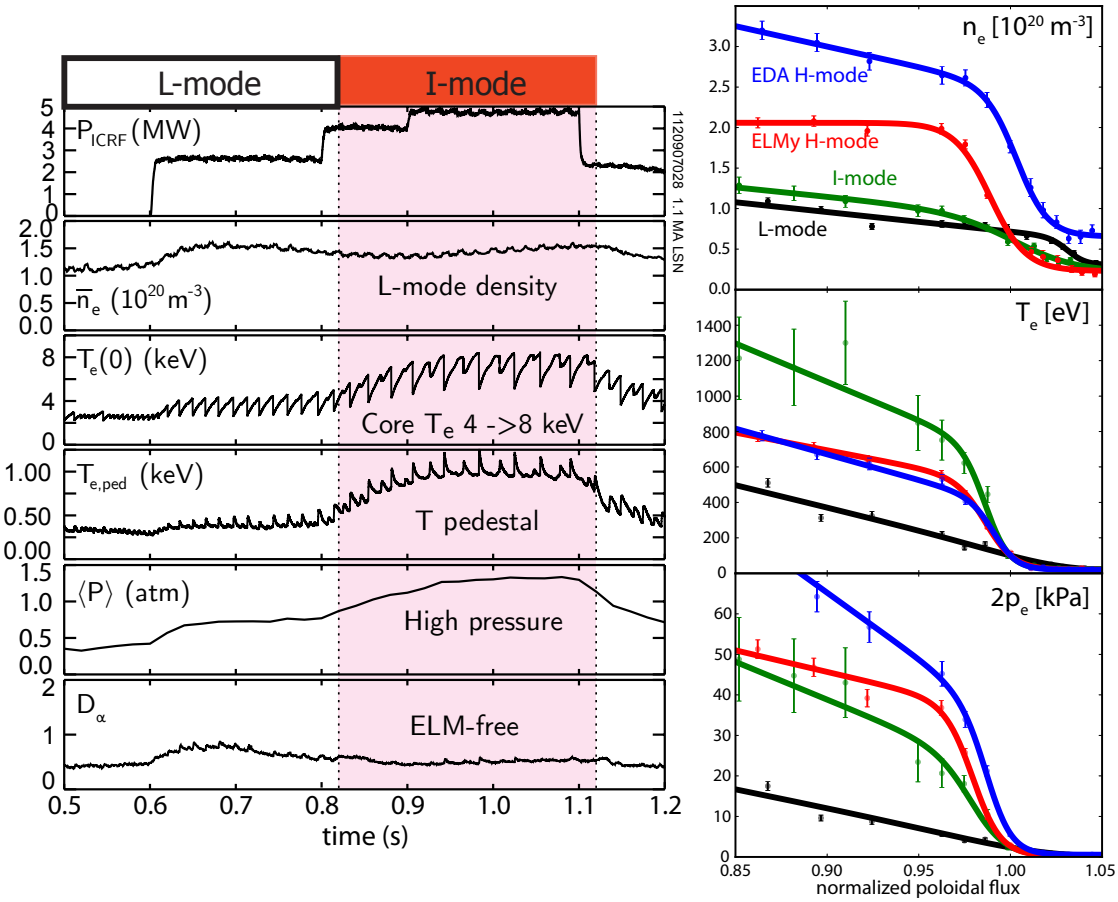

Figure 6: (left) Characteristic traces for a typical I-mode. At the L-I transition, the core and edge temperature rise over several sawtooth cycles before reaching a steady level; global confinement and pressure rise accordingly. However, the density remains at L-mode levels, and no ELMs are exhibited. (right) Edge profiles for density, temperature, and pressure in L-, I-, and H-mode. The I-mode (green) retains an density profile comparable to the L-mode (black), unlike the ELMy (red) and EDA (blue) H-modes which form a strong density pedestal. However, the I-mode forms a higher temperature pedestal than either H-mode. As a result, the I-mode reaches comparable pedestal pressures to the H-modes while retaining L-mode particle transport.

The temperature pedestal in I-mode exhibits some H-mode-like behavior, particularly in its response to plasma current $T_{e,ped} \sim I_p$. Notably, I-mode temperature pedestals typically exceed that in a comparable H-mode (albeit at lower density). This is highly beneficial for global performance, as high temperature pedestals support steep core temperature gradients via marginally-stable stiff temperature profiles, sustaining high core temperatures. Provided a moderate degree of density peaking,, this leads to comparable core and volume-averaged pressure to H-mode despite the comparatively reduced pedestal pressure in I-mode. The temperature pedestal responds strongly to heating power, $T_{e,ped} \sim P_{net}/\overline{n}_e$ (effectively, heating power per particle) at fixed current. This is distinct from the behavior in ELMy H-mode, for which the temperature responds only weakly to heating power (rather, elevated power tends to increase ELM-driven heat transport to maintain the limited $\beta_{p,ped}$ in the pedestal). Transport-limited EDA H-modes also exhibit a response in the pedestal temperature with power-per-particle, suggesting that I-mode pedestals are similarly not stability-limited.

ref if we include this

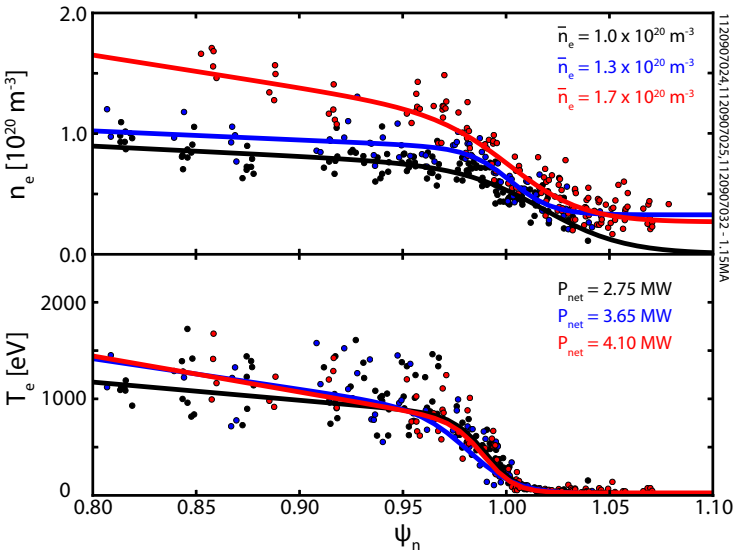

Figure 7: Density and temperature pedestals at matched current, field, and shaping, with varying fueling and heating power levels. The three discharges are fueled to $\overline{n}_e$ of 1.0 (black), 1.3 (blue), and 1.7×10^{20} m^{-3} (red) respectively, with heating powers of 2.75, 3.65, and 4.10 MW to maintain matched $P_{net}/\overline{n}_e \sim 2.4 - 2.7$. The constant power-per-particle maintains matched temperature pedestals across the fueling range, indicative of the independent control of pedestal n_e and T_e available in I-mode.

In contrast, the density profile is set by operator-controlled fueling, independent of the stability or transport-driven limits found in H-mode, due to the L-mode-like density profile. Given sufficient heating power to maintain $P_{net}/\overline{n}_e$, temperature pedestals are matched across a broad range of fueling (fig. 7). Fueling and heating power are thus largely-independent "knobs" for operator control of pedestal profiles, in contrast to both stability-limited ELMy H-mode pedestals (where the density and temperature are inversely proportional to maintain the fixed $\beta_{p,ped}$ limit) and EDA H-modes, where the den-

sity is locked to a transport-limited value set by the plasma current, insensitive to operator fueling.

The pressure pedestal reflects this beneficial behavior, scaling as $p_{ped} \sim I_p$ and $p_{ped} \sim P_{net}$ (consistent with the temperature scaling as $P_{net}/\overline{n}_e$ and $p_{ped} \sim n_{e,ped} T_{e,ped}$). The pedestal pressure is typically reduced compared to comparable H-modes due to the lower density, and exhibits a pressure gradient that is relaxed compared to H-mode, and trends more weakly than I_p^2, consistent with MHD stability in the pedestal and with the lack of large ELMs. The strong scaling with heating power is consistent with a lack of degradation of τ_E with heating power, distinct from the $\tau_E \sim P^{-0.7}$ expected for H-mode. This behavior is quite favorable when scaled to large, high-power machines, particularly in high-Q scenarios with significant fusion self-heating where the plasma pressure directly determines the heating power via the fusion reaction rate (proportional to p^2).

Pedestal Width

The pedestal width in I-mode appears to be quite robust, with no systematic trend with any of the examined physics parameters. In particular, no dependence on $\beta_{p,ped}$ is seen, in contrast to the expectation for pedestals limited by KBM turbulence, with I-mode pedestals consistently broader than predicted by an EPED-like relation (fig. 8). Similarly, no width dependence in the temperature or pressure pedestal is seen with gyroradius (thus ion-orbit-loss models), collisionality or safety factor (thus edge current and magnetic shear impact on MHD stability), or heat flux through the pedestal. The linear relationship between p_{ped} and ∇p across the I-mode dataset (fig. 9) suggests that MHD instability driven by the pressure gradient may still present an ultimate limit on the I-mode pedestal; however, the degree of operator control over pedestal profiles in I-mode will allow the operator to approach, but not exceed, the stability limit in the pedestal.

Global Confinement & Performance

Although the I-mode exhibits a more relaxed pressure pedestal (i. e., lower $\beta_{p,ped}$) compared to typical H-modes, the comparatively higher pedestal temperature supports steep core temperature profiles, reaching significant core and average pressure provided moderate density peaking. I-mode reaches comparable levels of global (normalized) pressure, $\langle \beta_N \rangle$, maintaining good energy confinement (see fig. 10), while the relaxed pressure pedestal provides beneficial stability and impurity-confinement properties.

The weak degradation of energy confinement with heating power is reflected in the stored energy, which scales as $W \sim P_{net} I_p$ – by definition $W \sim P\tau_E$, and from the H-mode confinement scaling one expects

Figure 8: Pedestal width versus poloidal beta in I-mode and ELMy H-mode. ELMy H-modes lie on the $\Delta_\psi \sim \beta_{p,ped}^{1/2}$ line predicted for KBM-limited pedestals. I-mode shows no scaling of the pedestal width with β_p, and exhibits pedestals consistently wider than predicted for comparable ELM-limited pedestals.

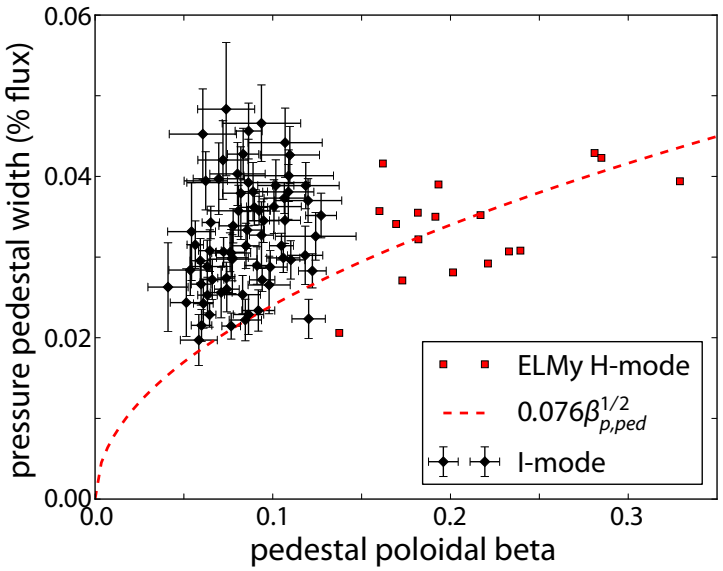

Figure 9: Peak ∇p in the I-mode pedestal versus p_{95}. There is a robust linear dependence between the pedestal gradient and height, consistent with a robust pedestal width.

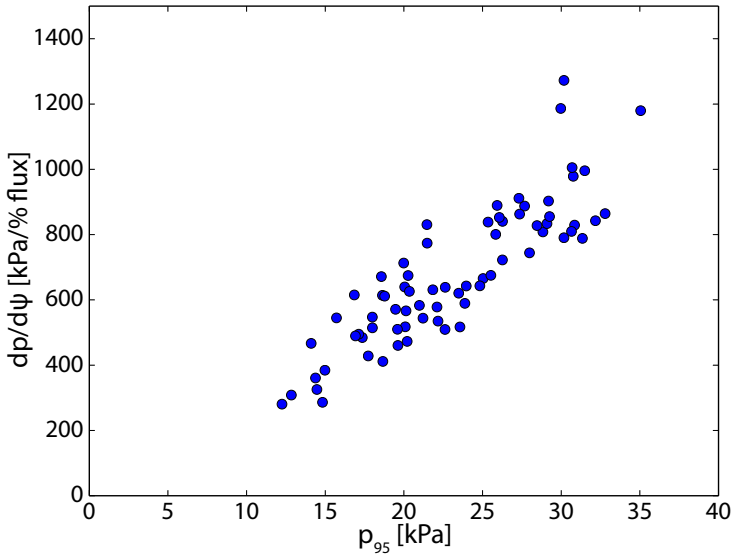

$\tau_E \sim I_p$. The $W \sim P_{net} I_p$ trend therefore indicates minimal dependence of τ_E on power, in contrast to the expected $W \sim P_{net}^{0.3} I_p$ for H-mode confinement. This is consistent with the pedestal response, $p_{ped} \sim P_{net}$ at fixed current (as the pedestal pressure strongly constrains the core, $W \sim p_{ped}$). The degradation of τ_E with heating power in H-mode reflects the MHD limits on the pedestal, for which increased heating power drives increased ELM heat transport to maintain the limited pedestal, in turn driving a weak increase in stored energy with heating power. Thus, the lack of degradation in I-mode is indicative of the inherent MHD stability of the pedestal. Similarly, the stored energy responds strongly to fueling, consistent with the strong pedestal response (provided sufficient heating power), in contrast to β_p-limited ELMy H-mode pedestals. Like the strong response

Figure 10: Global normalized β_N versus confinement factor H_{98} for I-mode and ELMy H-mode. Despite the relaxed pedestal pressure, I-modes reach comparable average pressures, while maintaining H-mode-like energy confinement.

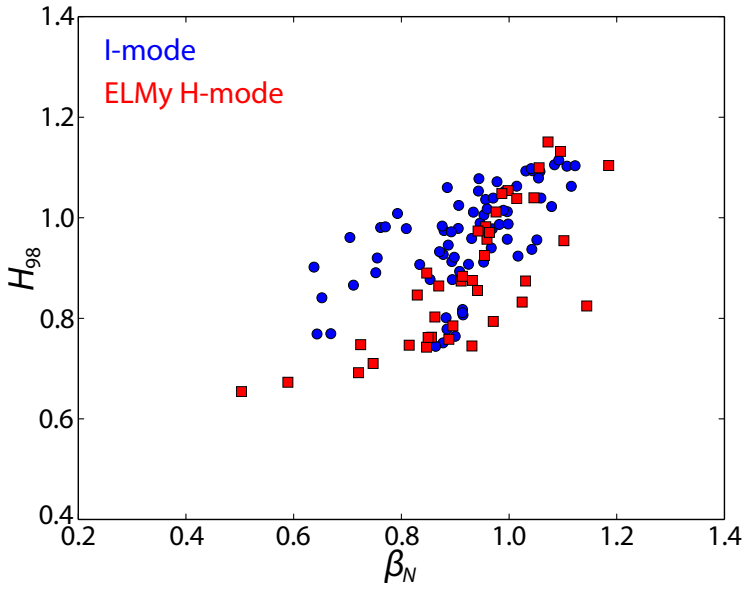

Figure 11: I-mode stored energy versus the product of net heating power P_{net} and plasma current I_p. Based on the H-mode confinement scaling, τ_E is expected to scale linearly with I_p, and to show a strong degradation with heating power: $\tau_E \sim I_p \times P_{net}^{-0.7}$. As the stored energy is given by $W \sim P_{net}\tau_E$, $W \sim I_p P_{net}^{0.3}$ is expected. The observed linear trend indicates little-to-no degradation of τ_E in I-mode with heating power.

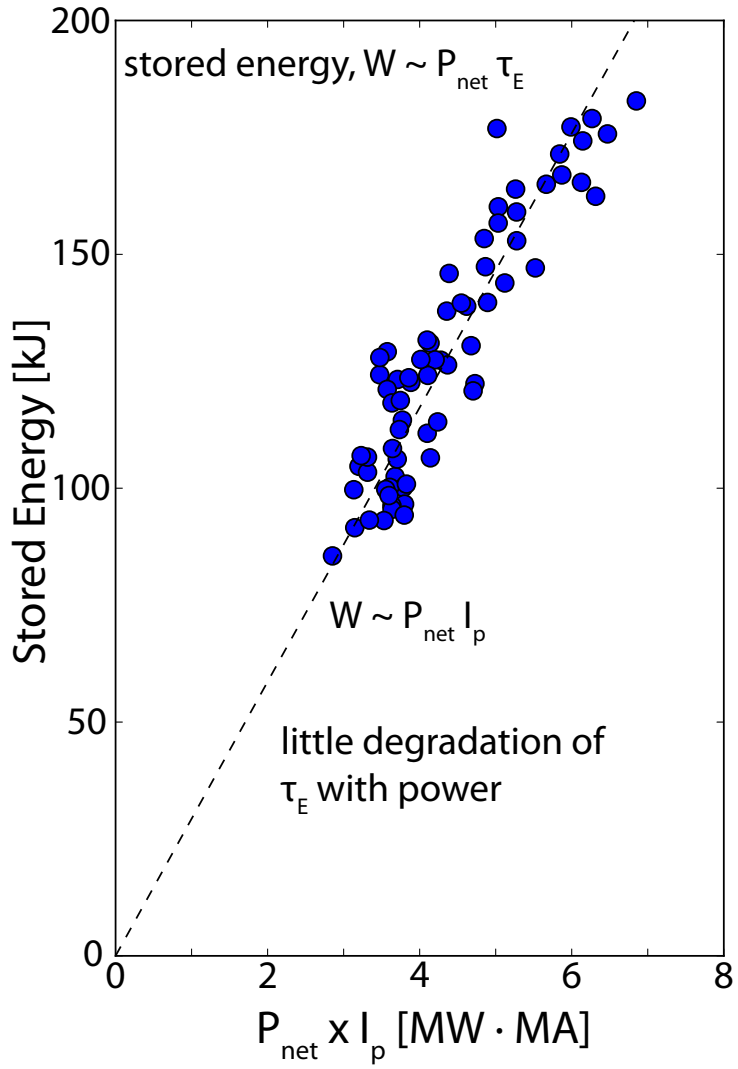

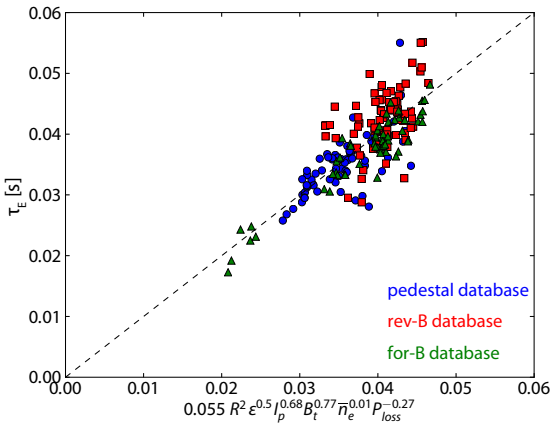

Figure 12: Power-law fit to I-mode energy confinement time τ_E, with the *ansatz* of an $R^2\sqrt{\varepsilon}$ size scaling fixed. Both the high-resolution pedestal database and older reversed-field LSN and forward-field USN I-mode databases are used. Note the expected weak degradation of τ_E with heating power.

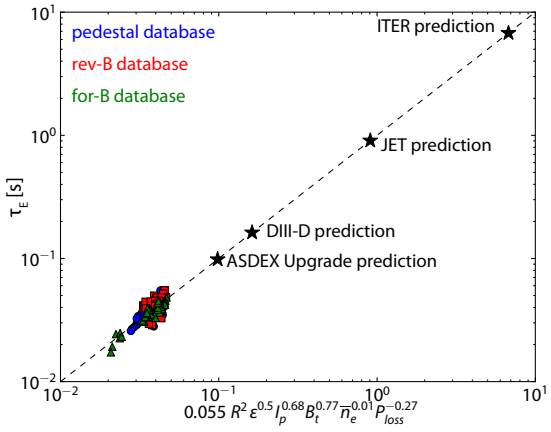

Figure 13: Modeled energy confinement time τ_E with the fixed $R^2\sqrt{\varepsilon}$ size scaling, extrapolated to DIII-D, ASDEX Upgrade, JET, and ITER. Modeled energy confinement times are competitive with H-modes, both the measured τ_E for existing machines and the expected ITER98y2 prediction for ITER H-modes.

to heating power, this is desirable for a burning-plasma scenario, in which heating power $\sim P_\alpha$ is proportional to the square of the plasma density.

An examination of the I-mode energy confinement time under a power-law fit of the form used for the ITER89 and ITER98 scalings for L- and H-mode is consistent with the observed behavior in I-mode, particularly capturing the weak degradation with heating power ($\tau_E \sim P^{-0.28}$), as shown in fig. 12 (note that this includes a fixed $R^2\sqrt{\varepsilon}$ size scaling assumed based on H-mode confinement – size-independent single-machine scalings for C-Mod data capture the same behavior, however). While this scaling is purely illustrative, as the examined parameter range is too restricted to confidently apply to other devices, such behavior would extrapolate to an energy confinement time of $\tau_E \sim 8$ s, well in excess of the $\tau_E \sim 2.5$ s expected for ITER in H-mode (fig. 13).

I-MODE STABILITY MODELING

FUTURE WORK

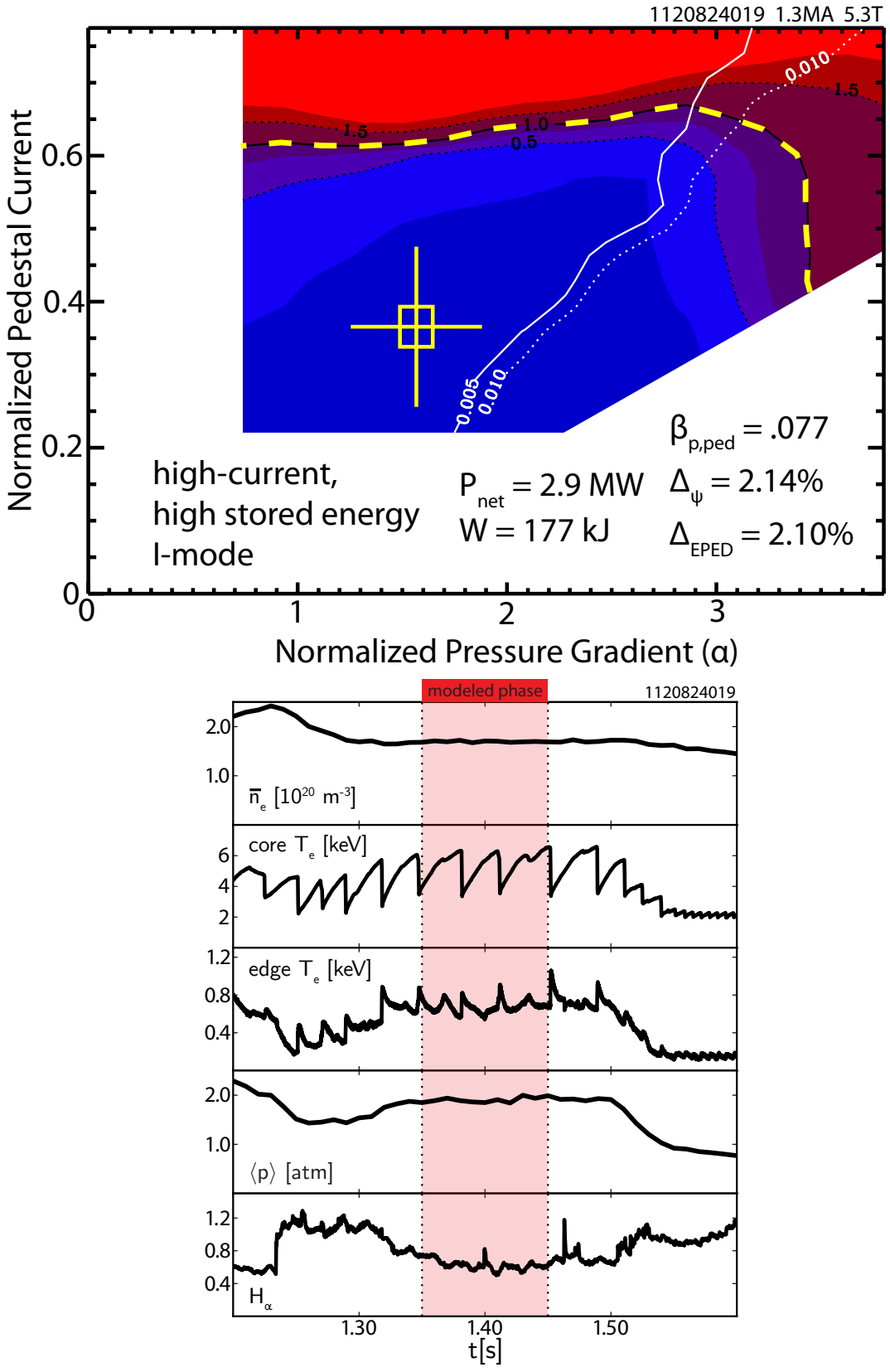

Figure 14: MHD stability contour for a high-current (1.3 MA), high-performance I-mode generated by the ELITE code, with KBM threshold calculated by BALOO overlaid. The experimental measurement is shown by the crosshair, with the stability boundary indicated by the yellow dashed line. Parameters for the modeled phase of the discharge are shown below. The I-mode pedestal is observed to be far from both the peeling and ballooning MHD stability boundaries, as well as below the KBM threshold (0.01, indicated by the dotted line)

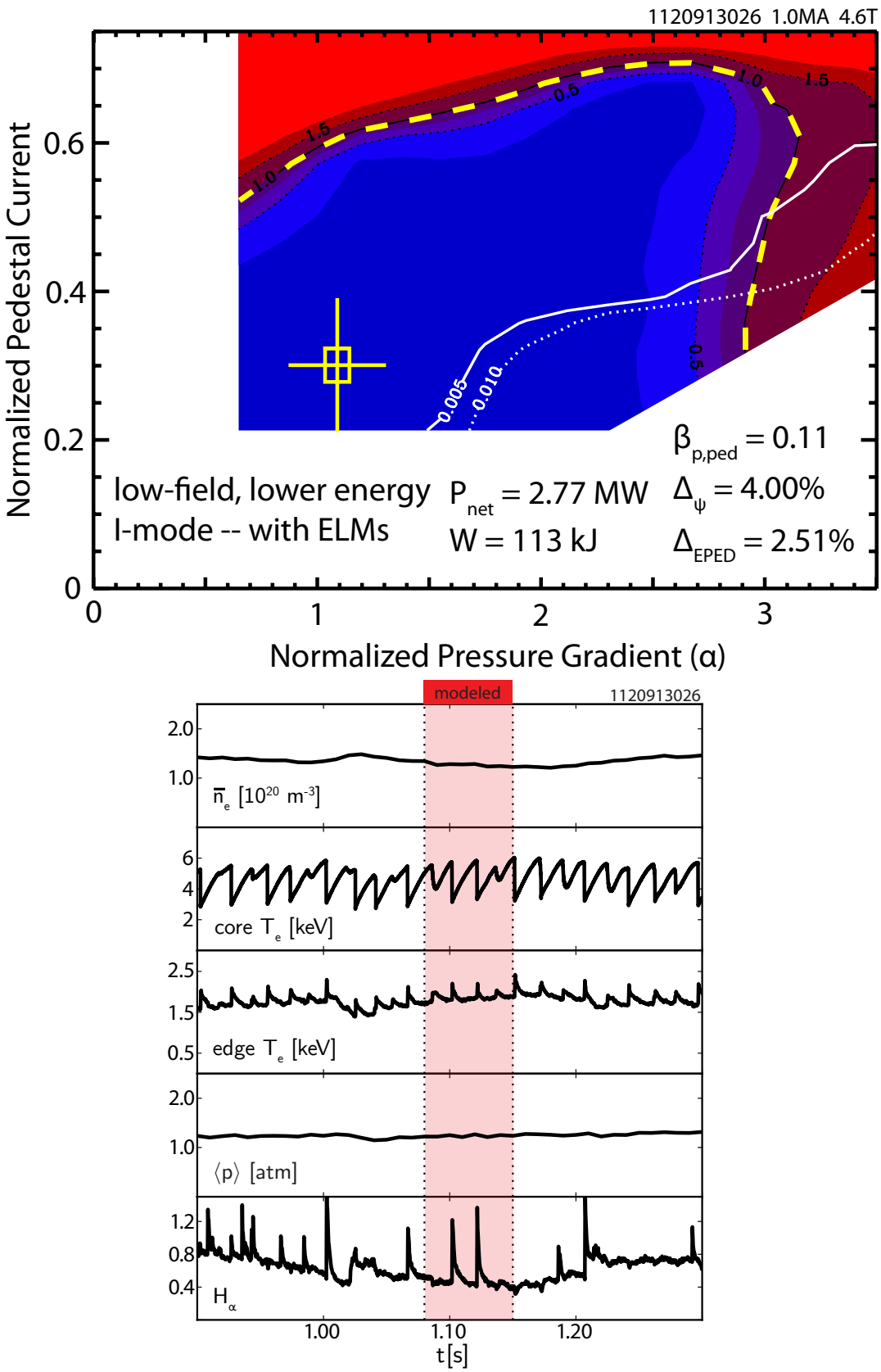

Figure 15: MHD stability contour for a low-field (4.6 T), lower-energy I-mode generated by the ELITE code, with KBM threshold calculated by BALOO overlaid. The experimental measurement is shown by the crosshair, with the stability boundary indicated by the yellow dashed line. Parameters for the modeled phase of the discharge are shown below. This case exhibited small,intermittent ELM-like events, but is still calculated to be peeling-ballooning stable and below the KBM threshold (0.02) for profiles averaged over the time window.

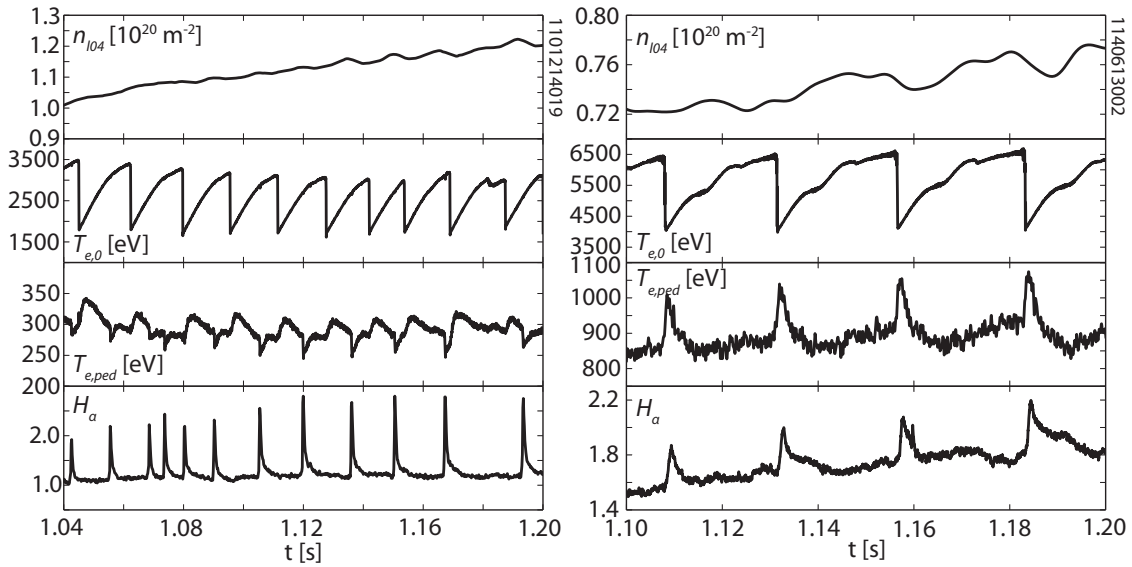

Figure 16: Traces of n_{l04}, core and edge ($r/a \sim 0.98$) T_e, and H_α for ELMy H-mode (left) and I-mode (right). ELMs in H-mode (visible on the H_α trace) are independent of the sawtooth cycle, and drive perturbations to the edge temperature and line-integrated density, as both energy and particles are expelled form the plasma by the ELM crash. This is particularly clear on the edge temperature, which exhibits a clear increase with the sawtooth heat pulse and a separate crash with the ELM. I-mode, in contrast, exhibits ELMs (or ELM-like events) that are tied to sawtooth heat pulses reaching the edge, as visible on the ECE T_e signal. No visible crash in edge temperature is visible following the ELM, nor is there a significant perturbation to the density.

BIBLIOGRAPHY

[1] M. Shimada, D.J. Campbell, V. Mukhovatov, M. Fujiwara, N. Kirneva et al. Chapter 1: Overview and summary. *Nuclear Fusion*, 47(6):S1, 2007.

[2] D.G. Whyte, A.E. Hubbard, J.W. Hughes, B. Lipschultz, J.E. Rice et al. I-mode: an H-mode energy confinement regime with L-mode particle transport in Alcator C-Mod. *Nuclear Fusion*, 50(10):105005, 2010.

[3] J.R. Walk, P.B. Snyder, J.W. Hughes, J.L. Terry, A.E. Hubbard et al. Characterization of the pedestal in Alcator C-Mod ELMing H-modes and comparison with the EPED model. *Nuclear Fusion*, 52(6):063011, 2012.

[4] R.J. Groebner, C.S. Chang, J.W. Hughes, R. Maingi, P.B. Snyder et al. Improved understanding of physics processes in pedestal structure, leading to improved predictive capability for ITER. *Nuclear Fusion*, 53(9):093024, 2013.

[5] J. R. Walk, J. W. Hughes, A. E. Hubbard, J. L. Terry, D. G. Whyte et al. Edge-localized mode avoidance and pedestal structure in I-mode plasmas. *Physics of Plasmas*, 21(5):–, 2014.

[6] P.B. Snyder, R.J. Groebner, J.W. Hughes, T.H. Osborne, M. Beurskens et al. A first-principles predictive model of the pedestal height and width: development, testing and ITER optimization with the EPED model. *Nuclear Fusion*, 51(10):103016, 2011.

[7] J.W. Hughes, P.B. Snyder, J.R. Walk, E.M. Davis, A. Diallo et al. Pedestal structure and stability in H-mode and I-mode: a comparative study on Alcator C-Mod. *Nuclear Fusion*, 53(4):043016, 2013.